Journal of the Serbian Chemical Society

JSCS-info@shd.org.rs • www.shd.org.rs/JSCS

J. Serb. Chem. Soc. 76 (7) 1027–1035 (2011)
JSCS–4181

UDC 669.112.227/.228:620.193:
669.14.018.8:621.791
Original scientific paper

Corrosion of an austenite and ferrite stainless steel weld

VLADANA N. RAJAKOVIĆ-OGNJANOVIĆ[1]* and BRANIMIR N. GRGUR[2]

[1]Institute of Hydraulic and Environmental Engineering, Faculty of Civil Engineering, University of Belgrade, Bulevar kralja Aleksandra 73, 11 000 Belgrade and [2]Department of Physical Chemistry and Electrochemistry, Faculty of Technology and Metallurgy, University of Belgrade, Karnegijeva 4, 11 000 Belgrade, Serbia

(Received 26 July, revised 25 December 2010)

Abstract: Dissimilar metal connections are prone to frequent failures. These failures are attributed to the difference in the mechanical properties across the weld, the coefficients of thermal expansion of the two types of steels and the resulting creep at the interface. For the weld analyzed in this research, it was shown that corrosion measurements can be used for a proper evaluation of the quality of weld material and for the prediction of whether or not the material, after the applied welding process, can be in service without failures. It was found that the corrosion of the weld analyzed in this research resulted from the simultaneous activity of different types of corrosion. In this study, electrochemical techniques including polarization and metallographic analysis were used to analyze the corrosion of a weld material of ferrite and austenitic stainless steels. Based on surface, chemical and electrochemical analyses, it was concluded that corrosion occurrence was the result of the simultaneous activity of contact corrosion (ferrite and austenitic material conjuction), stress corrosion (originating from deformed ferrite structure) and inter-granular corrosion (due to chromium carbide precipitation). The value of corrosion potential of –0.53 V shows that this weld, after the thermal treatment, is not able to repassivate a protective oxide film.

Keywords: welding; corrosion; stainless steel.

INTRODUCTION

The welding of dissimilar metals is a very challenging task due to differences in physical, mechanical and metallurgical properties of the parent metals. In order to take full advantage of the properties of different metals, it is necessary to achieve reliable welds between them. The growing availability of new materials and the higher requirements being placed on materials creates a greater need for

* Corresponding author. E-mail: vladana@grf.bg.ac.rs
doi: 10.2298/JSC100726090R

joints and welds of dissimilar metals. When welding ferrite stainless steels, the problem of coarse grains in the weld zone and heat affected zone of fusion welds are encountered with the consequence of low toughness and ductility due to the absence of phase transformation during which grain refinement can occur.[1] When welding austenitic stainless steels, susceptibility to hot cracking in the weld metal and heat-affected zone is of major concern. This cracking occurs primarily due to low-melting liquid phases that allow boundaries to separate under thermal and shrinkage strains during weld solidification and cooling. Austenitic stainless steel welds exhibit some degree of susceptibility to localized corrosion, pitting and crevice corrosion, and in many cases, it is the limiting factor in stainless applications.[2–9] It is generally accepted that delta ferrite when present in small amounts in an austenite matrix is detrimental to pitting resistance as it provides favorable sites for pitting initiation in the weld metal. The corrosion problems commonly associated with welding of austenitic stainless steels are related to both precipitation effects and chemical segregation. The microstructure of the solidified fusion zone of a weld is always subject to segregation during solidification. There are some differences in segregation for different solidification modes of the weld metal. Welding of ferritic to austenitic stainless steels is considered to be a major problem due to difference in coefficient of thermal expansion, which may lead to crack formation at the interface, formation of hard zone close to the weld interface, relatively soft regions adjacent to the hard zone; large hardness difference between the hard and the soft zones and expected differences in microstructure may lead to failures in service. Solid state welding is a possible solution to these problems.[3] For the weld material analyzed in this research, it was shown that detailed microstructural examination and electrochemical and corrosion measurements can be used for the proper evaluation of the quality of the weld material and for the prediction of whether or not the material after the applied welding process could be in service without failures.

EXPERIMENTAL

Materials and welding processes

The nominal chemical compositions of the stainless steel (STS) samples with ferrite and austenite structure used for the welding process are given in Table I.

TABLE I. Nominal chemical composition of used stainless steel materials in mass %

STS Structure	Cr	C	Si	Mn	Ni
Ferrite (X6Cr17)	16.50	0.05	0.35	0.40	–
Austenite (X5CrNi18-10)	18.10	0.04–0.05	0.50	1.10–1.50	8.30–9.20

Welding of austenite and ferrite stainless steel was performed using cooled water and round Cu–Cr electrodes with a contact surface of constant diameter of 1 mm. Welding was performed by placing metal sheets (100 cm^2) in the sample holder. Before welding, the plates were clamped on each end to a heavy backing fixture to prevent deformation.

Characterization techniques

Chemical analysis. Chemical analysis of the materials was performed by the X-Ray fluorescent spectroscopy (XRF) technique using excitation sources of ^{109}Cd and ^{241}Am, according to a modified EPA 6200 method.[10] The quantitative chemical analysis of samples (dissolved in an acidic solution) was performed by atomic absorption spectroscopy (AAS). All results are shown as a mean value of three independent measurements, with a precision of ±0.01 %.

Optical examinations. Optical examination of samples was realized using a NIKON DIC microscope. The "Photoshop" computer program was used to analyzed the microstructure of the pure and welded materials. Before optical examination, the welded material was treated for 72 h in a 3 % solution of NaCl, with the addition of HCl (pH 4). All samples were prepared according to known metallographic procedures, which included mirror polishing and etching in hydrofluoric acid.

Electrochemical corrosion measurements. Electrochemical techniques were applied in order to define the corrosion behavior of all the investigated materials. A three-compartment glass cell was used. Surface area (A) of the working electrodes of pure austenite and ferrite stainless steel was 2 cm^2. Working electrodes of welded stainless steels near the weld (A = = 1 cm^2) was prepared by cutting the austenite and ferrite samples near the weld from the large size (100 cm^2) welded samples. The reference electrode was saturated calomel (SCE, all potentials are reffered to SCE), while the counter electrode was a platinum foil. A mild steel sample was used for comparison.[11,12] The experiments were performed in a 3 % solution of NaCl, with the addition of HCl, to adjust the pH to 4.00 at 25 °C. The corrosion current density was estimated from the intercept of the cathodic slope of the polarization curve with the corrosion potentials. For all electrochemical experiments a potentiostat/galvanostat PAR M273 was used.

RESULTS AND DISCUSSION

Chemical analysis

The XRF spectrum of the austenite and ferrite weld is shown in Fig. 1. XRF Spectrum of this material showed the presence of Cr, Fe, Ni and Mo. As can be seen, the amount of Fe was the highest, then Cr and Ni in small amounts, and finally traces of Mo and Cu in amounts typical for trace elements.

AAS Techniques and clasical gravimetric methods were used to determine the chemical compositions of the used stainless steels. The obtained results are given in Table II.

The results of the XRF and gravimetric analyses for the quantitative determination of the composition of the materials showed that the contents of Cr and Mn were lower than expected, as well as the content of Si in the ferrite sample. AAS Analysis indicated the presence of Ni (0.17 %) in the ferrite sample. The content of carbon and organic impurities according to the AAS measurements was high. The content of carbon was expected to be up to 0.05 %, but according to the chemical analysis it was much higher. Higher contents of carbon and organic impurities, as well as the lower chromium content, were probably the main reason for the appearance of corrosion, especially in ferrite material, resulting from chromium carbide precipitation during the welding.

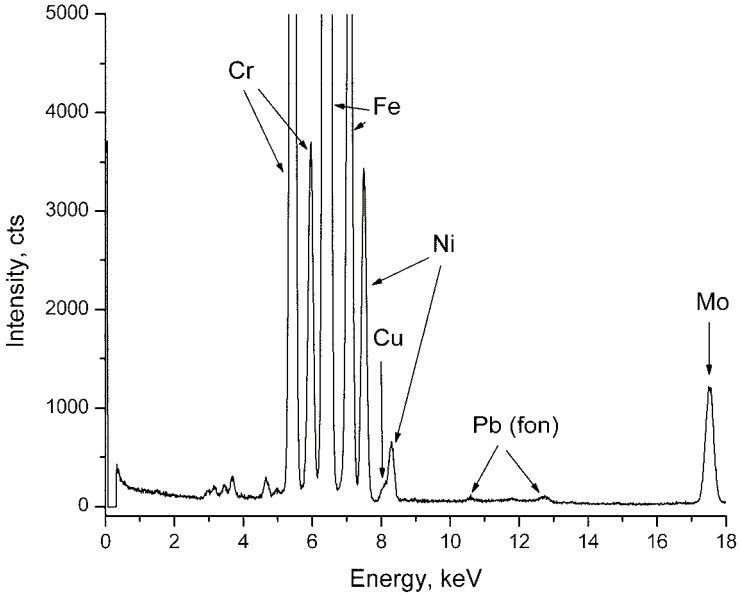

Fig. 1. XRF Spectrum of the austenite and ferrite weld.

TABLE II. Determined chemical composition of the used stainless steel materials in mass %

STS Structure	Cr	Si	Mn	Ni	C
Ferrite	15.5	<0.001	0.30	0.17	0.20–0.5
Austenite	17.8	0.40	1.10	8.00	0.20

Microstructural analysis

Microstructural analysis of ferrite stainless steel. The microstructure of analyzed ferrite stainless steel sample is shown in Fig. 2. The microstructure is not homogenous at the intersection, as shown in the microphotographs of Fig. 3a. The structure consists of ferrite seeds and carbide particles. More than half of the analyzed intersection consists of ferrite seeds, which are polygonal, uniform in size, and have a small-seeded structure, as shown in Fig. 2a. The carbide particles, as shown in Fig. 2b, have a small-seeded structure, globular shape, and were formed between the ferrite seeds.

Microstructural analysis of austenitic stainless steel. The microstructure of the analyzed austenitic stainless steel sample is shown in Fig. 3. The microphotograph at the intersection of this material shows its homogeneous structure, with rough seeds. The size of austenitic seeds is mostly uniform, as shown in Fig. 3a, but there are some very rough seeds, as shown in Fig. 3b.

Microstructural analysis of the weld. A microphotograph of the ferrite and austenite stainless steel weld is shown in Fig. 4. The ferrite material is in the upper part and the austenitic material is in the lower part of the image.

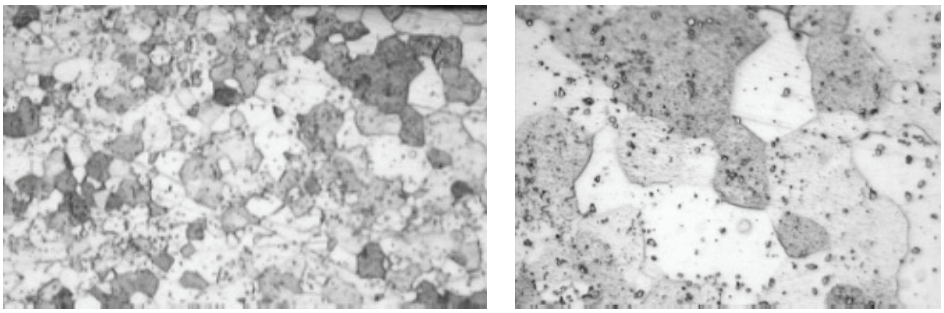

(a) (b)

Fig. 2. Microphotographs of the ferrite stainless steel sample. Magnification: a) 200×; b) 500×.

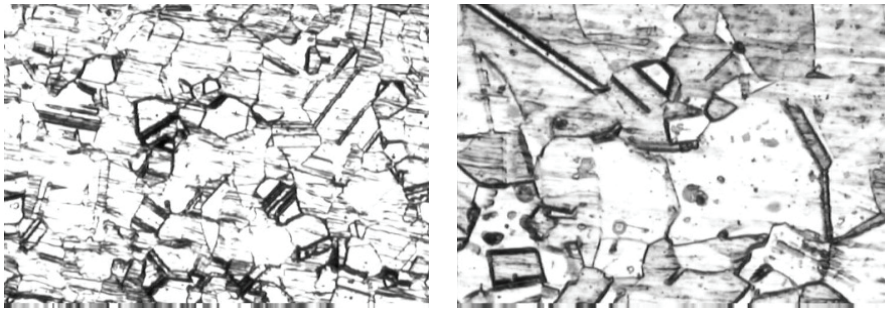

(a) (b)

Fig. 3. Microphotographs of the austenitic stainless steel sample. Magnification: a) 500×; b) 400×.

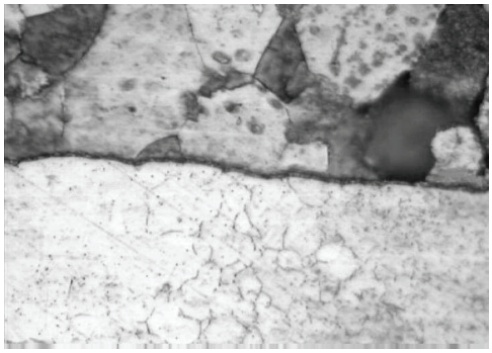

Fig. 4. Microphotograph of the weld sample. Magnification: 500×.

The micrographs of the ferrite part of the analyzed weld sample revealed the existence of inter-granular corrosion, as shown in Fig. 5. This could be connected with precipitation of chromium carbide during the thermal treatment.

When analyzing the microphotographs of the ferrite part near the weld, at a lower magnification, some indications of stress corrosion could be observed, as shown in Fig. 6a and 6b.

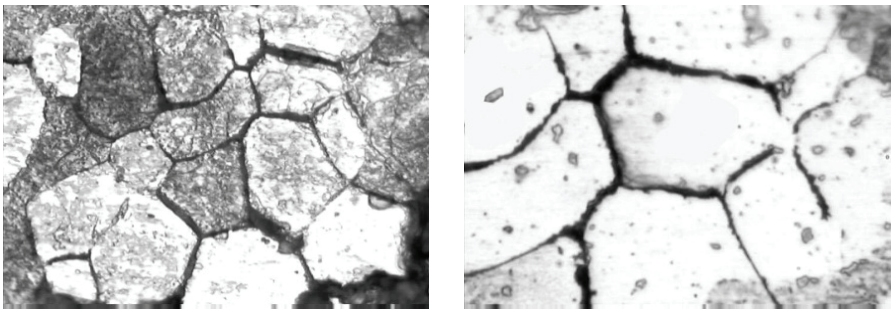

(a) (b)

Fig. 5. Microphotographs of the ferrite part near the weld. Magnification: a) 500×; b) 1000×.

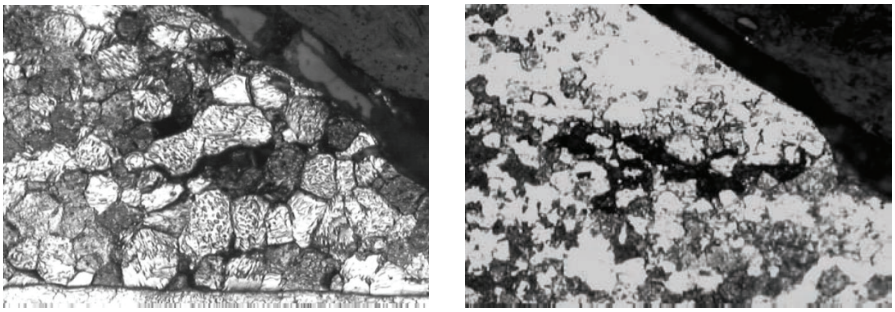

(a) (b)

Fig. 6. Microphotographs of ferrite part near the weld with indication of stress corrosion. Magnification: 200×.

Electrochemical measurements

Electrochemical properties of basic materials. The polarization experiments were performed in a solution simulating the aggressive solution in which the final product could be used.[13] The polarization curves of the ferrite and austenite materials are shown in Fig. 7, together with that of a mild steel sample, shown for comparison.

Both analyzed samples of stainless steel were practically in the passive state with corrosion potentials of approximately –0.2 V. The value obtained for the mild steel in the same solution was –0.53 V, which could be used for comparison. The estimated corrosion current density was 0.08 for austenite and 0.10 μA cm^{-2} the ferrite sample. In comparison, the corrosion current density for the mild steel was 20 μA cm^{-2}.[14]

Corrosion resistance properties of the welded material. The polarization curves for the ferrite and austenitic part of the weld sample are shown in Fig. 8. The austenitic part of the analyzed weld sample remained practically unchanged during welding, according to the metallographic analysis. Even the corrosion potential was unchanged, as presented in Fig. 8. This part has some structural

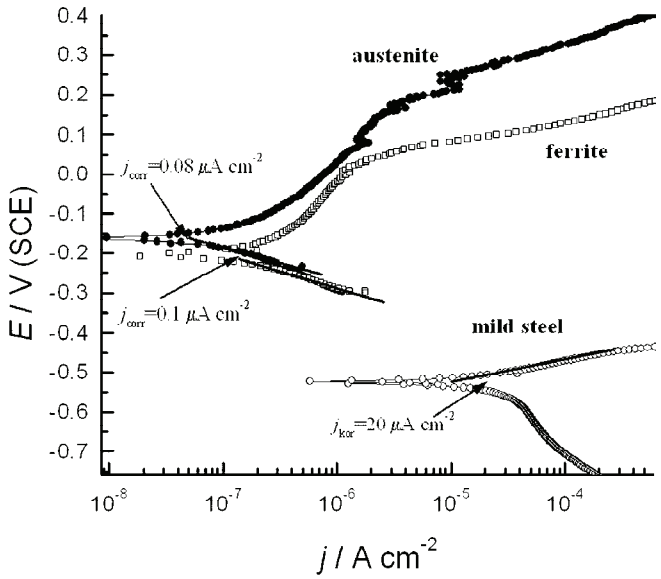

Fig. 7. Polarization curves of the analyzed materials before welding compared to mild steel in 3 % NaCl solution at pH 4.00.

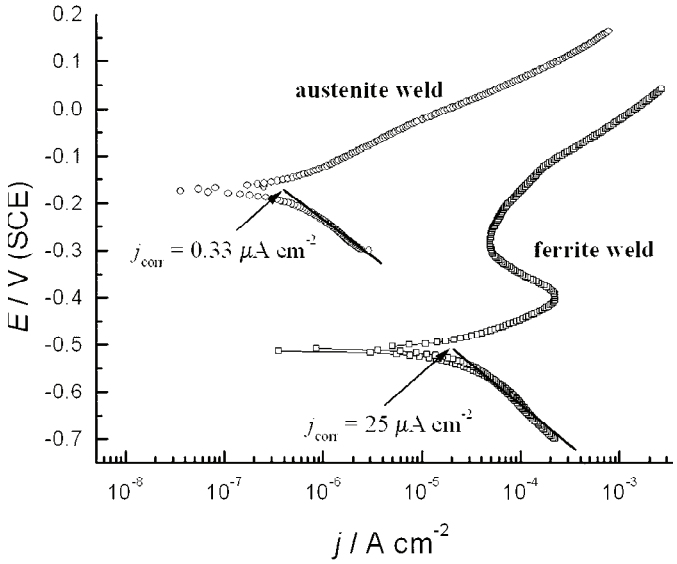

Fig. 8. Polarization curves of the austenitic and ferrite part of the weld sample in 3 % NaCl solution at pH 4.00.

changes which provoke an increase in the estimated corrosion current density. On the other hand, the characteristics of the ferrite material were changed significantly. The corrosion potential of –0.53 V implies that this material after thermal

treatment did not show the ability to repassivate a protective oxide film. The estimated corrosion current density was approximately 75 times higher. This implies that the basic ferrite material was degraded by uncontrolled thermal treatment during the welding process, with the formation of a deformed ferrite structure.[15,16]

CONCLUSIONS

Using the XRF and AAS analytical techniques, it was shown that austenite and ferrite stainless steel had a different chemical composition than the nominal composition. A smaller content of chromium and a higher content of carbon were found than declared. Both materials exhibited relatively good corrosion resistance before welding.

For the ferrite and austenite stainless steel weld analyzed in this study, it was shown that detailed a microstructural examination and electrochemical corrosion measurements could be used for a proper evaluation of the quality of the weld material. With a thorough analysis of the materials used for welds, a prediction of whether the material could be in service without failures can be made.

The weld analyzed in this research showed a tendency towards contact corrosion due to the inadequate welding processes. The corrosion was the result of stress corrosion (from deformation of the basic ferrite structure), and inter-granular corrosion (from carbide precipitation and applied welding method). When improved, the welding process could significantly prevent the appearance of corrosion.

Acknowledgements. The support of the Research Fund of Serbia is gratefully acknowledged.

ИЗВОД

КОРОЗИЈА ЗАВАРЕНОГ СПОЈА АУСТЕНИТНОГ И ФЕРИТНОГ НЕРЂАЈУЋЕГ ЧЕЛИКА

ВЛАДАНА Н. РАЈАКОВИЋ-ОГЊАНОВИЋ[1] и БРАНИМИР Н. ГРГУР[2]

[1]Институт за хидротехнику и водно–еколошко инжењерство, Грађевински факултет, Универзитет у Београду, Булевар краља Александра 73, 11 000 Београд и [2]Катедра за физичку хемију и електрохемију, Технолошко–металуршки факултет, Универзитет у Београду, Карнегијева 4, 11 000 Белоград

Спојеви различитих метала добијених заваривањем склони су пропадању углавном услед појаве различитих видова корозије. Физичко–хемијска, механичка својства, као и коефицијенти топлотног ширења различитих челика најчешћи су узрок пуцања материјала на завареним спојевима. Истраживања у овом раду су показала да се испитивање корозије материјала може користити за процену квалитета спојева заварених материјала. Различите аналитичке, металографске и електрохемијске технике и методе анализе су примењене за испитивање корозије завареног споја нерђајућих челика феритне и аустенитне структуре. Установљено је да до појаве корозије на завареном споју испитиваних материјала превасходно долази услед: контактне корозије, напонске корозије (која потиче од деформисане структуре ферита) и међукристалне корозије (последица излуживања хром-карбида) у феритном делу завареног споја.

(Примљено 26. јула, ревидирано 25. децембра 2010)

REFERENCES

1. I. Serre, J. B. Vogt, *Mater. Design* **30** (2009) 3776
2. Y. Cui, C. D. Lundin, *Mater. Design* **28** (2007) 324
3. V. V. Satyanarayana, G. R. Madhusudhan, T. Mohandasb, *J. Mater. Process. Technol.* **160** (2005) 128
4. A. Joseph, S. K. Rai, T. Jayakumar, N. Murugan, *Int. J. Press. Vessels Pip.* **82** (2005) 700
5. T. G. Gooch, *Weld. J.* **75** (1996) 135
6. B. T. Lu, Z. K. Chen, J. L. Luo, B. M. Patchett, Z. H. Xu, *Corrosion Eng. Sci. Tech.* **38** (2003) 69
7. Z. Fang, Y. Wu, R. Zhu, *Corrosion* **50** (1994) 873
8. D. Rodriguez-Marek, M. Pang, D. F. Bahr, *Metall. Mater. Trans. A* **34** (2003) 1291
9. B. T. Lu, Z. K. Chen, J. L. Luo, B. M. Patchett, Z. H. Xu, *Electrochim. Acta* **50** (2005) 1391
10. EPA 2600, *Method 6200: Field portable X-ray fluorescence spectrometry for the determination of elemental concentrations in soil and sediment*, 2007, http://www.epa.gov/osw/hazard/testmethods/sw846/pdfs/6200.pdf (not anymore accessible)
11. M. M. Popović, B. N. Grgur, V. B. Mišković-Stanković, *Prog. Org. Coat.* **52** (2005) 359
12. V. B. Mišković-Stanković, D. M. Dražić, Z. Kačarević-Popović, *Corrosion Sci*. **38** (1996) 1513
13. M. Kabasakaloglu, I. Kalyoncu, T. Kiyakt, *Appl. Surf. Sci.* **135** (1998) 188
14. ASTM International, *ASTM A 380-99: Standard Practice for Cleaning, Descaling, and Passivation of Stainless Steel Parts, Equipment and Systems*, 2001, http://www.astm.org/DATABASE.CART/HISTORICAL/A380-99E1.htm (accessed July 2011)
15. Hascalik, E. Unal, N. Ozdemir, *J. Mater. Sci.* **41** (2006) 3233
16. J. Wang, C. Li, H. Liu, H. Yang, B. Shen, S. Gao, S. Huang, *Mater. Charact.* **56** (2006) 73.